Simulated Hydrologic Response to Projected Changes in Precipitation and Temperature in the Congo River Basin

Supplementary Information

1. Congo River Basin Hydrology Model

We use the Soil Water Assessment Tool [*Arnold et al.*, 1998], a physically-based, semi-distributed, watershed-scale model that operates at a daily time step, to simulate the hydrological processes in the Congo River Basin (CRB). The spatial heterogeneities are incorporated by dividing the river basin into smaller watersheds (n=1,575) and further dividing these watersheds into hydrologic response units (HRUs, n~8,500) based on land cover (16 classes) [*Bartholomé and Belward*, 2005], soils (150 types) [*FAO/IIASA*, 2009] and topography (90m digital elevation model) [*H Lehner et al.*, 2008]. Gridded, one degree latitude /longitude horizontal resolution, daily values of minimum and maximum temperature and precipitation for the period 1948-2008 are used as climate inputs [*Sheffield et al.*, 2006]. The water balance in each HRU is calculated separately and aggregated at watershed level. Each watershed consists of one stream section to which the generated runoff (surface, lateral and groundwater) is routed. The runoff accumulated in each stream section is routed through the stream network using the variable storage routing method [*Neitsch et al.*, 2011]. We also include the wetlands and lakes (Figure 1A in the main text), which regulate the river flows at various locations, as unregulated storage reservoirs. A wetland is modeled as a storage structure that intercepts runoff only within the watershed where it is located, and is positioned off the stream section. Whereas, lakes (n=16, Table S1) receive water from all the upstream watersheds and are located on the stream [*Neitsch et al.*, 2011]. The potential evapotranspiration (PET) is estimated by Hargreaves method [*Hargreaves and Riley*, 1985]. The overland flow, percolation through the soil zone and lateral flow are modeled using the Soil Conservation Service curve number method (SCS-CN), a storage routing and a kinematic storage model, respectively [*Arnold et al.*, 1998; *Neitsch et al.*, 2011; *USDA Soil Conservation Service*, 1972]. In SCS-CN method, overland flow (q_s) is defined as $q_s = \frac{(R-\lambda S)^2}{(R-(1-\lambda)S)}$ when $R > \lambda S$ and $q_s = 0$ otherwise, where R is the daily rainfall, S is the retention parameter which varies due to changes in soil type, land cover, slope and changes in soil water content and λ is the initial abstraction ratio. The value of S is transformed to the curve number (CN) by the formulation $S = 25.4\left(\frac{1000}{CN} - 10\right)$. Recent studies suggest that the value for λ should more appropriately be near 0, as opposed to SWAT adopted value of 0.2 [*Hawkins et al.*, 2009; *Lamont et al.*, 2008]. In this study we set $\lambda = 0.01$, and the curve numbers for different land cover types were estimated by calibration. The relationship between water-spread area of lakes and the corresponding storage volume is modeled as $A = aV^b$, where, A and V are area and volume, and a and b are parameters estimated by calibration. The relationship between outflows from the lakes and the storage volume is modeled as $q_l = a_1 V^{b_1}$, where, q_l is the outflow from lakes and a_1 and b_1 are parameters estimated by calibration. The nonlinear groundwater storage and discharge response at HRU level is modeled as q= $\sqrt[(2-b_2)]{\left((2-b_2)a_2(S-S_o)\right)}$, where q is the groundwater contribution to the total runoff generated within an HRU, S is the shallow aquifer storage and S_o is the minimum aquifer storage required for groundwater flow and a_2 and b_2 (< 2.0) are parameters (see similar approach in *Kirchner* [2009]). Values for S_o, a_2 and b_2 are estimated by calibration.

Accessible streamflows (AF), at monthly time steps were estimated by applying baseflow filter technique described in *Nathan and McMahon* [1990].

2. Temporal Downscaling of Climate Variables

We use three-hourly and monthly observed climate fields [*Sheffield et al.*, 2006] and bias-corrected monthly climate fields to temporally downscale the bias-corrected three-hourly fields, following the method described in *Sheffield et al.* [2006]. The precipitation fields are scaled as follows:

$$P_{BC,3hr} = \frac{P_{BC,mon}}{P_{Obs,mon}} \times P_{Obs,3hr} \quad (1)$$

where P is precipitation, *3hr* and *mon* indicate three-hourly and monthly values, and *BC* and *Obs* indicate bias-corrected GCM simulations and observations, respectively. The three-hourly values are summed to obtain daily precipitation.

The temperature values are disaggregated to three-hourly values using a two-step procedure, in order to scale with the monthly mean temperature and the diurnal temperature range, as follows:

$$T_{BC,3hr} = T_{Obs,3hr} + \left(T_{BC,mon} - T_{Obs,mon}\right) \quad (2)$$

$$T_{BC,3hr} = T_{BC,daily} + \frac{DTR_{BC,mon}}{DTR_{Obs,mon}} \times \left(T_{BC,3hr} - T_{BC,daily}\right) \quad (3)$$

where T and DTR are temperature and diurnal temperature range, respectively. The daily average temperature used in (3) is computed from the three-hourly temperature in (2). The daily minimum and maximum temperatures are extracted from the three-hourly values computed in (3).

Supplementary Tables

Table S1 Area, volume and annual mean precipitation in lakes used in this study.

Lake Name (Latitude/Longitude)	Area (km^2)	Volume (km^3)	Average annual rainfall[1] (mm)	Key references
Bangweulu (11.8S, 29.9E)	3,900	8.2	1,300	*Burgis and Symoens [1987]*, *Lehner and Döll* [2004], *Serruya and Pollingher* [1983] and *Tilzer and Serruya* [1990]
Kabamba (7.8S, 26.9E)	170	2.6	1,360	*Lehner and Döll* [2004]
Kabele (8.8S, 26.2E)	100	5.7	1,600	*Lehner and Döll* [2004]
Kabwe (9.0S, 26.0E)	100	1.9	1,200	*Lehner and Döll* [2004]
Kisale (8.1S, 26.8E)	260	7.2	1,600	*Lehner and Döll* [2004]
Kivu (2.5S, 28.9E)	2,500	570	1,300	*Lehner and Döll* [2004], *Lempicka* [1971], *Serruya and Pollingher* [1983] and *Tilzer and Serruya* [1990]
Mai Ndombe (2.7S, 18.1E)	2,200	11.4	1,600	*Lehner and Döll* [2004], *Serruya and Pollingher* [1983] and *Tilzer and Serruya* [1990]
Mwadingusha (10.7S, 27.3E)	410	1	1,030	*Lehner and Döll* [2004], *Magis* [1961] and *Serruya and Pollingher* [1983]
Mweru (8.5S, 28.8E)	4,700	38	1,100	*Bos et al.* [2006], *Lehner and Döll* [2004], *Serruya and Pollingher* [1983] and *Tilzer and Serruya* [1990]
Mweru Wantipa	1,450	8	1,100	*Burgis and Symoens [1987]*, *Lehner and Döll* [2004], *Tilzer*

(9.0S, 29.4E)				*and Serruya* [1990]
Nzilo (10.4S, 25.4E)	230	2	1,100	*Crul* [1992], *Lehner and Döll* [2004], *Serruya and Pollingher* [1983] and *Magis* [1961]
Tanganyika (5.9S, 29.1E)	32,000	18,900	1,100	*Lempicka* [1971], *Lehner and Döll* [2004], *Serruya and Pollingher* [1983] and *Tilzer and Serruya* [1990]
Tele (1.1S, 17.0E)	23	0.071	1,600	[*Laraque et al.*, 1998] and *Lehner and Döll* [2004]
Tumba (0.6S, 17.8E)	610	3	1,540	*Burgis and Symoens [1987]*, *Lehner and Döll* [2004], *Serruya and Pollingher* [1983] and *Tilzer and Serruya* [1990]
Upemba (8.4S, 26.4E)	550	1.3	1,600	*Burgis and Symoens [1987]*, *Lehner and Döll* [2004], *Serruya and Pollingher* [1983] and *Tilzer and Serruya* [1990]
Zimbambo (8.0S, 27.0E)	200	4.8	1,600	*Lehner and Döll* [2004]

[1]annual average rainfall in the watershed where the lake is located

Table S2 Global Climate Model outputs used in this study

Model Number	Model Name	Institute
M1	ACCESS1-3	Commonwealth Scientific and Industrial Research Organisation (CSIRO) and Bureau of Meteorology (BOM), Australia
M2	bcc-csm1-1	Beijing Climate Center, China
M3	BNU-ESM	GCESS, BNU, Beijing, China
M4	CanESM2	Canadian Center for Climate Modeling and Analysis, Canada
M5	CCSM4	National Center for Atmospheric Research, USA
M6	CESM1-CAM5	National Center for Atmospheric Research, USA
M7	CNRM-CM5	Centre National de Recherches Meteorologiques, France
M8	CSIRO-Mk3-6-0	CSIRO Marine and Atmospheric Research, Australia
M9	EC-EARTH	European Earth System Model, EU
M10	FIO-ESM	The First Institution of Oceanography, SOA, Qingdao, China
M[11-13]	GISS-E2-H*	Goddard Institute for Space Studies, USA
M[14-16]	GISS-E2-R*	Goddard Institute for Space Studies, USA
M17	HadGEM2-CC	Met Office Hadley Centre, UK
M18	HadGEM2-ES	Met Office Hadley Centre, UK
M19	INM-CM4	Institute for Numerical Mathematics, Russia
M20	IPSL-CM5A-LR	Institut Pierre Simon Laplace, France
M21	MIROC5	Japan Agency for Marine-Earth Science and Technology (JAMSTEC), Atmosphere and Ocean Research Institute, The University of Tokyo, and National Institute for Environmental Studies, Japan
M22	MIROC-ESM	Japan Agency for Marine-Earth Science and Technology (JAMSTEC), Atmosphere and Ocean Research Institute, The University of Tokyo, and National Institute for Environmental Studies, Japan

M23	MPI-ESM-LR	Max Planck Institute for Meteorology, Germany
M24	MRI-CGCM3	Meteorological Research Institute, Japan
M25	NorESM1-M	Norwegian Climate Centre, Norway

*these climate models provide outputs from three different physics ensembles. We treat each a separate model.

Table S3 Annual and season values of precipitation and runoff in the CRB and four regions identified in Figure 1 in the main text for the reference period 1986-2005. The values are based on the multi-model mean (n=25). All values in mm per year/season.

	Congo (CRB)	Northern (NC)	Equatorial (EQ)	Southwestern (SW)	Southeastern (SE)
Precipitation					
Annual	1,439	1,453	1,599	1,359	1,110
DJF	368	34	332	505	561
MAM	410	356	464	419	307
JJA	219	582	280	16	4
SON	442	481	523	418	239
Runoff					
Annual	382	241	515	410	125
DJF	103	31	134	133	49
MAM	103	17	130	151	53
JJA	71	68	103	55	10
SON	105	126	149	72	13

Table S4 projected changes in precipitation (%) in the CRB and four regions for the near-term (2016-2035) and the mid-term (2046-2065) relative to the reference period of 1986-2005 (REF). The regions are identified in Figure 1A in the main text. Number of GCMs used in the multi-model mean is 25. The interquartile range across the 25 GCM-simulations is provided in parenthesis. DJF: Dec-Jan-Feb, MAM: Mar-Apr-May, JJA: Jun-Jul-Aug and SON: Sep-Oct-Nov.

	RCP45					RCP85				
	Congo (CRB)	Northern (NC)	Equatorial (EQ)	Southwestern (SW)	Southeastern (SE)	Congo (CRB)	Northern (NC)	Equatorial (EQ)	Southwestern (SW)	Southeastern (SE)
Near-term (2016-2035)										
Annual	1.1 (2.7)	1.7 (3.5)	1.3 (3.5)	1.3 (2.8)	-0.4 (4.3)	1.0 (1.7)	1.3 (3.1)	1.1 (1.7)	1.5 (2.5)	0.1 (4.6)
DJF	1.2 (2.9)	3.3 (20.7)	2.0 (4.6)	1.6 (3.1)	-0.3 (3.9)	1.1 (4.0)	5.4 (19.7)	1.4 (5.4)	1.8 (4.6)	0.0 (5.4)
MAM	0.7 (3.4)	1.4 (5.9)	0.5 (4.4)	1.5 (4.4)	-0.5 (8.5)	1.2 (4.3)	1.1 (5.5)	0.8 (4.2)	2.5 (4.8)	0.9 (9.5)
JJA	1.3 (4.0)	1.3 (3.8)	1.3 (5.2)	-0.7 (14.5)	19.6 (45.5)	1.0 (4.9)	0.4 (4.1)	1.3 (4.6)	-0.3 (14.7)	18.7 (35.1)
SON	1.4 (2.4)	2.3 (3.0)	1.7 (4.7)	0.9 (3.9)	-0.6 (8.2)	0.9 (4.1)	2.3 (6.8)	1.1 (3.9)	0.2 (4.9)	-1.0 (4.7)
Mid-Term (2046-2065)										
Annual	1.7 (2.6)	1.6 (4.1)	1.7 (2.7)	2.9 (3.7)	0.2 (7.2)	2.1 (5.8)	1.2 (8.2)	2.4 (4.7)	3.3 (3.8)	0.3 (9.6)
DJF	3.2 (6.4)	1.1 (21.8)	3.5 (6.5)	4.8 (6.2)	1.5 (7.3)	4.2 (11.2)	3.9 (21.6)	5.4 (8.1)	5.4 (10)	1.4 (10.7)
MAM	1.7 (4.0)	0.9 (5.1)	1.5 (4.6)	4.1 (5.0)	0.4 (8.4)	3.0 (3.5)	0.6 (7.3)	2.4 (3.5)	6.9 (9.1)	2.0 (15.9)
JJA	0.6 (5.6)	0.6 (5.7)	0.7 (9.5)	-6.1 (18.4)	6.7 (33.7)	1.4 (6.2)	0.1 (5.9)	2.2 (7.4)	-5.9 (18.2)	9.7 (33.3)
SON	0.9 (3.4)	3.4 (3.0)	1.3 (4.0)	-0.3 (3.8)	-3.2 (4.9)	-0.1 (4.9)	2.9 (11.8)	0.6 (6.3)	-2.5 (3.3)	-4.6 (4.5)

Table S5 projected changes in runoff (%) in the CRB and four regions for the near-term (2016-2035) and the mid-term (2046-2065) relative to the reference period of 1986-2005. The regions are identified in Figure 1A in the main text. Number of GCMs used in the multi-model mean is 25. The interquartile range between the 25 GCM-simulations is provided in parenthesis. DJF: Dec-Jan-Feb, MAM: Mar-Apr-May, JJA: Jun-Jul-Aug and SON: Sep-Oct-Nov.

	RCP45					RCP85				
	Congo (CRB)	Northern (NC)	Equatorial (EQ)	Southwestern (SW)	Southeastern (SE)	Congo (CRB)	Northern (NC)	Equatorial (EQ)	Southwestern (SW)	Southeastern (SE)
Near-term (2016-2035)										
Annual	4.8 (7.3)	3.6 (12.5)	5.0 (8.1)	5.6 (4.9)	1.4 (16.8)	4.5 (5.1)	2.5 (10.7)	4.3 (6.9)	6.0 (6.1)	4.2 (15.5)
DJF	5.3 (8.1)	5.7 (8.7)	6.3 (7.1)	4.2 (5.5)	1.3 (10.8)	4.6 (9.2)	6.0 (18.0)	5.1 (6.2)	3.9 (5.5)	2.8 (12.8)
MAM	5.4 (6.4)	9.4 (21.7)	5.5 (7.5)	6.3 (5.0)	0.4 (22.2)	6.2 (5.4)	9.1 (10.4)	5.7 (5.2)	7.7 (5.5)	4.4 (22.3)
JJA	3.8 (5.4)	2.6 (17.9)	3.4 (7.6)	6.7 (5.6)	2.8 (24.4)	4.2 (7.5)	1.9 (10.6)	3.8 (5.6)	7.7 (5.5)	8.3 (23.5)
SON	4.5 (7.8)	2.9 (9.9)	4.6 (7.4)	6.0 (5.4)	4.3 (11.4)	3.0 (9.1)	1.1 (13.2)	3.1 (9.0)	5.0 (9.2)	5.1 (10.2)
Mid-Term (2046-2065)										
Annual	6.6 (6.6)	1.2 (11.4)	6.3 (8.1)	9.9 (7.4)	6.1 (23.3)	7.2 (10.9)	-2.0 (21.9)	7.2 (10.2)	10.4 (8.4)	8.3 (28.5)
DJF	8.5 (8.8)	4.0 (7.6)	8.9 (9.1)	9.6 (11.3)	4.7 (24.3)	9.5 (18.8)	1.7 (32.0)	10.7 (15.9)	9.0 (17.1)	6.2 (36.2)
MAM	9.6 (6.5)	10.1 (14.2)	8.9 (7.0)	11.7 (7.7)	6.5 (31.4)	11.3 (10.1)	9.5 (15.5)	10.3 (6.0)	13.7 (9.9)	9.9 (39.8)
JJA	5.6 (7.8)	0.0 (18.2)	5.2 (8.6)	11.8 (10.0)	9.5 (37.3)	7.4 (9.8)	-2.5 (19.9)	7.5 (10.4)	13.7 (10.0)	14.9 (45.1)
SON	2.6 (8.9)	0.0 (15.3)	2.5 (7.5)	5.7 (7.6)	5.6 (9.5)	0.6 (10.9)	-4.1 (26.0)	1.1 (10.2)	3.3 (8.1)	3.1 (13.6)

Table S6 projected changes in runoff (%) in selected regions (within the four regions identified in Figure 1) for the near-term (2016-2035) and the mid-term (2046-2065) relative to the reference period of 1986-2005. The approximate locations are identified by latitudes and longitudes. Number of GCMs used in the multi-model mean is 25. The interquartile range between the 25 GCM-simulations is provided in parenthesis. DJF: Dec-Jan-Feb, MAM: Mar-Apr-May, JJA: Jun-Jul-Aug and SON: Sep-Oct-Nov.

	RCP45			RCP85		
	Northeast (3N-9N and 24E-30E)	Equatorial west (3S-3N and 18E-22E)	Southern sub region (8S-13S and 24E-32E)	Northeast (3N-9N and 24E-30E)	Equatorial west (3S-3N and 18E-22E)	Southern sub region (8S-13S and 24E-32E)
Near-term (2016-2035)						
Annual	-3.7 (19.0)	-0.7 (9.0)	-9.7 (31.8)	-6.6 (20)	-0.6 (6.8)	-10.1 (33.6)
DJF	6.5 (17.7)	2.7 (14.3)	-6.7 (23.1)	5.3 (29.1)	2.0 (8.0)	-6.3 (11.5)
MAM	-1.3 (18.4)	-0.5 (6.6)	-11.6 (34.7)	-3.9 (21.1)	-0.4 (8.6)	-10.8 (40.9)
JJA	-8.7 (17.2)	-3.9 (10.7)	-11.7 (32.4)	-11.3 (18.3)	-2.8 (13.3)	-10.9 (37)
SON	-2.0 (14.7)	0.0 (7.3)	-8.1 (29.2)	-5.1 (18.2)	-0.6 (12)	-12.1 (31.6)
Mid-Term (2046-2065)						
Annual	-5.1 (25.6)	-3.4 (7.4)	-13.9 (48.9)	-10.2 (24.2)	-2.4 (15.5)	-15.6 (55.4)
DJF	1.8 (38.4)	1.1 (8.9)	-9.9 (28.2)	-3.1 (44.3)	5 (16.4)	-9.9 (39.3)
MAM	6.7 (26.6)	-1.4 (6.7)	-15.2 (59.2)	7.0 (33.3)	-1.0 (9.5)	-15.9 (72.9)
JJA	-8.6 (18.2)	-5.8 (8.1)	-16.2 (55.6)	-12.1 (24.3)	-5.1 (20.5)	-17.9 (64.6)
SON	-5.5 (24.1)	-5.0 (7.5)	-16.8 (34.4)	-12.0 (23.8)	-5.1 (12.2)	-19.1 (39.1)

Supplementary Figures

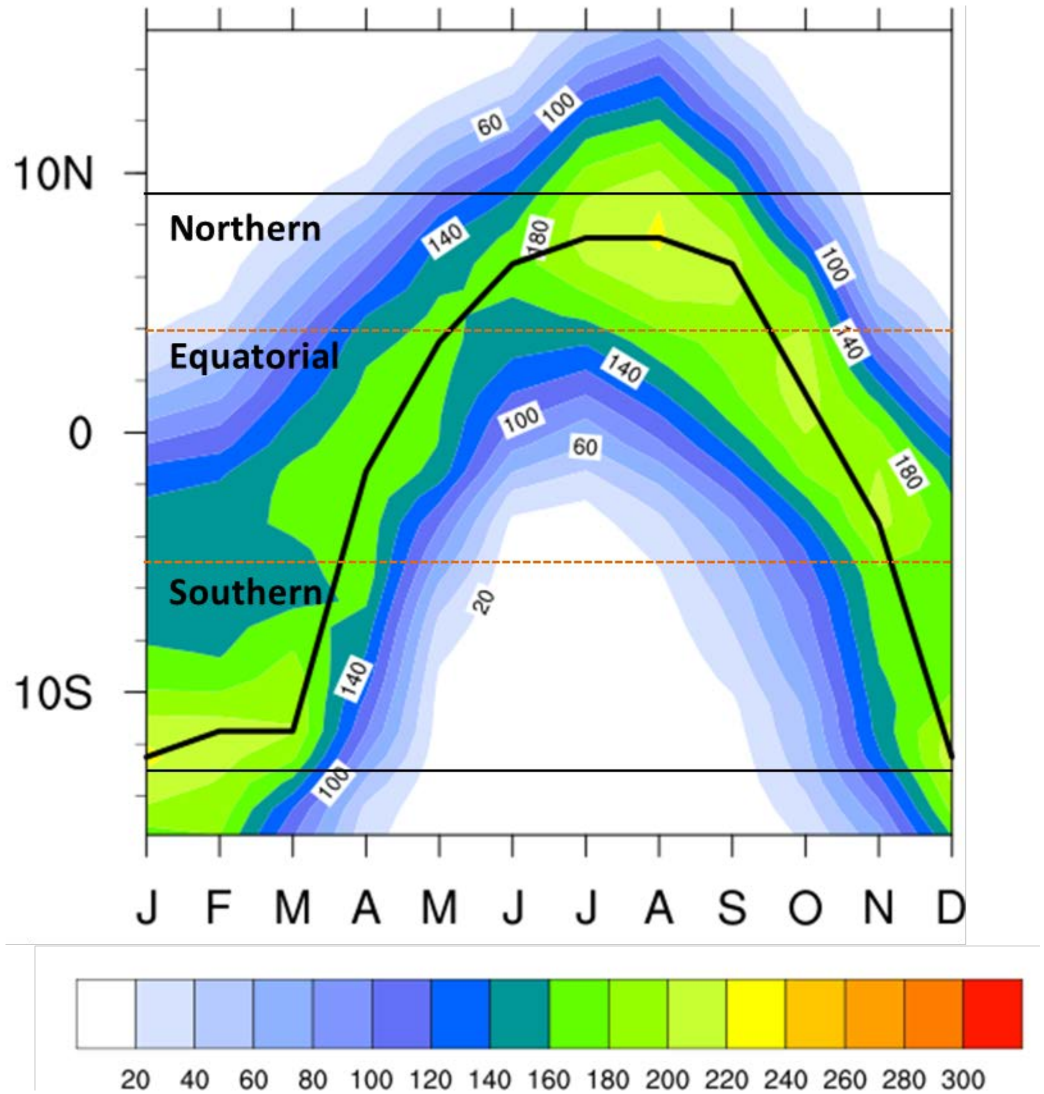
10N
0
10S
Northern
Equatorial
Southern
60
100
140
180
20
J F M A M J J A S O N D
20 40 60 80 100 120 140 160 180 200 220 240 260 280 300

Figure S1 Zonally (11.5^{o}E – 34.5^{o}E) averaged monthly precipitation over Central Africa. Monthly values are 1971-2000 averages obtained from *Sheffield et al.* [2006]. The black horizontal lines show the latitudinal boundaries of the Congo River Basin. The red dotted lines separate the Northern, Equatorial and Southern regions identified in Figure 1A in the main text.

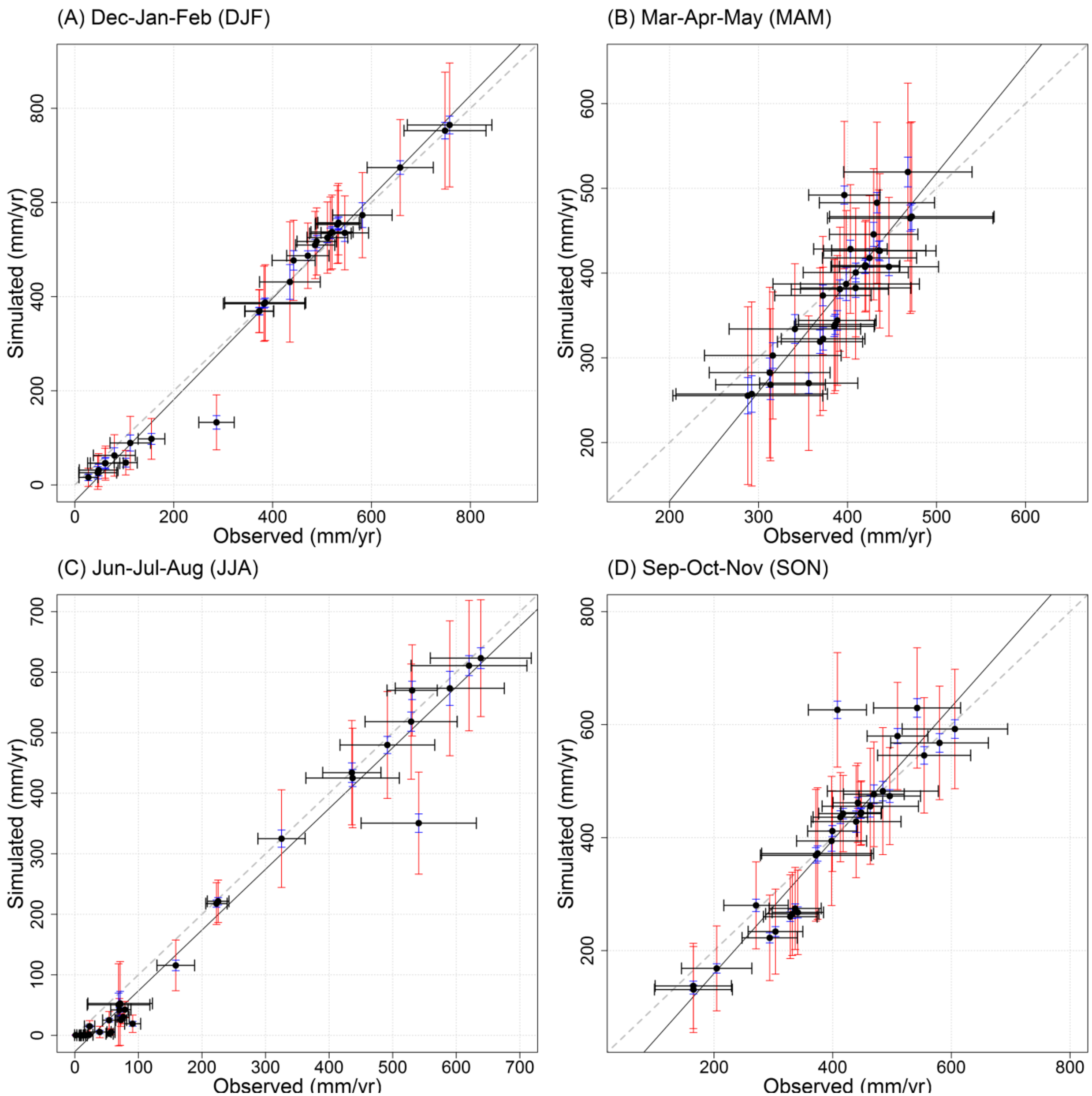
(A) Dec-Jan-Feb (DJF)
(B) Mar-Apr-May (MAM)
(C) Jun-Jul-Aug (JJA)
(D) Sep-Oct-Nov (SON)
Simulated (mm/yr)
Observed (mm/yr)

Figure S2 Observed and GCM-simulated seasonal precipitation averaged over the catchment areas of 30 stream flow gages in Figure 1A in the main text: (A) Dec-Jan-Feb, (B) Mar-Apr-May, (C) Jun-Jul-Aug and (D) Sep-Oct-Nov). Black dots compare multi-model means with observed precipitation, black horizontal bars show observed inter-annual variability, and red (blue) vertical bars show maximum (minimum) range of modeled inter-annual variability among the 25 climate model outputs.

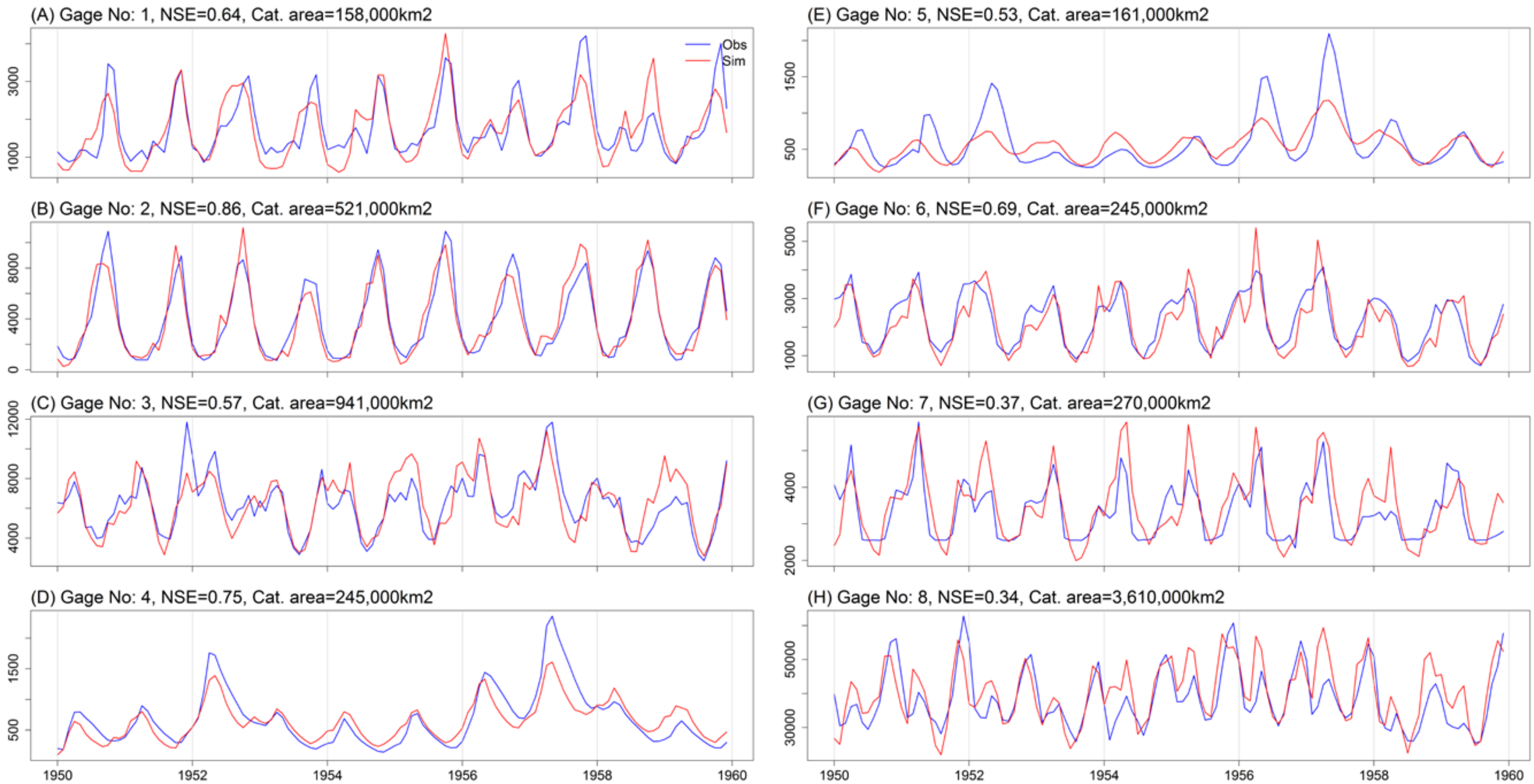

Figure S3 Monthly stream flow hydrographs at selected locations in Figure 1A for the period 1950-1959, the blue (red) lines are observed (simulated) flows. NSE – Nash-Sutcliff model efficiency values, a measure of relative magnitude of residual variance compared to the observed flow variance, and catchment areas above each gage are also given. Monthly mean flows are in m3/s.

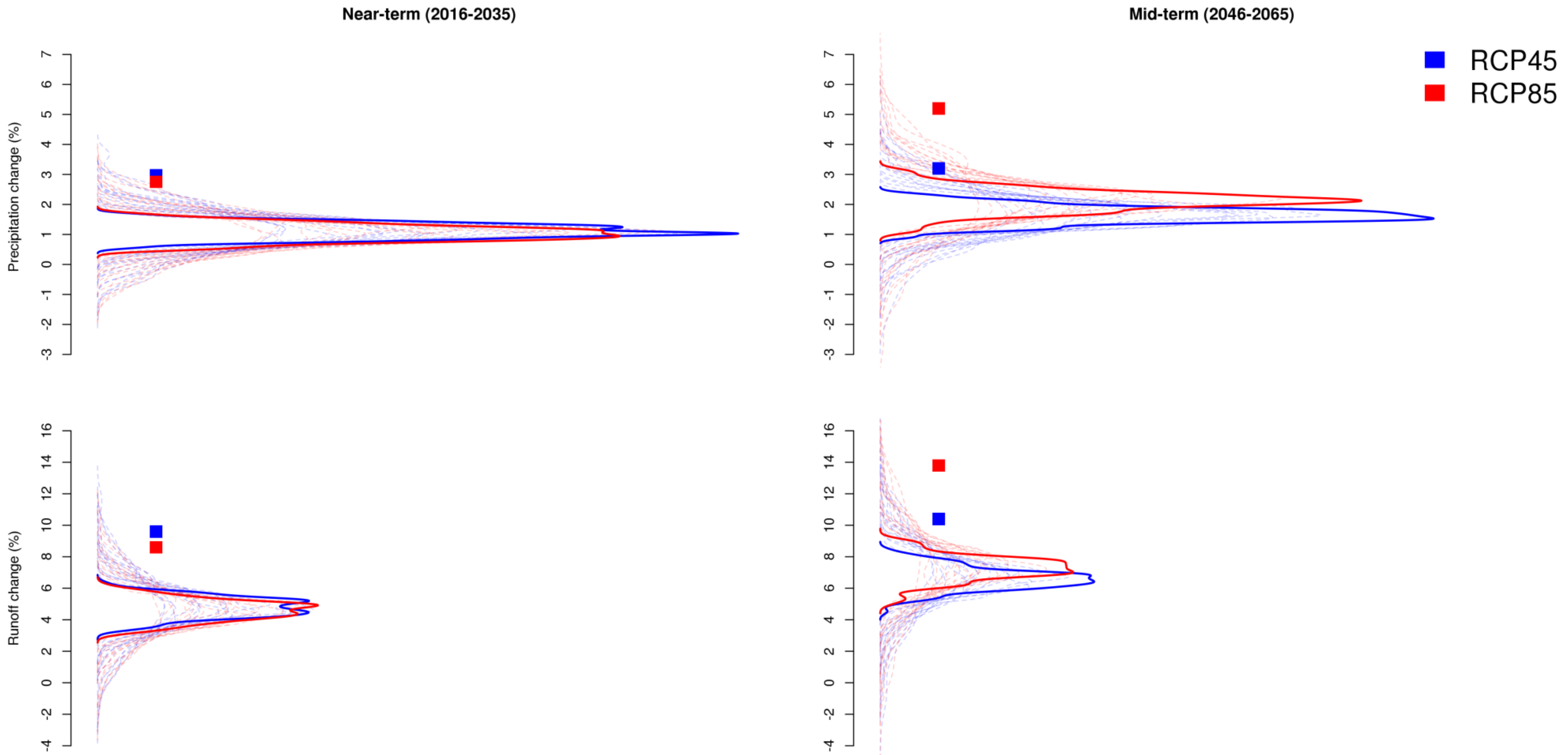

Figure S4 Multi-model ensemble means computed using randomly sampled GCM simulations from the available 25. The thick blue (red) curves show the distribution of multi-model means for 20 randomly sampled simulations for RCP45 (RCP85) emission scenario. The dotted blue (red) lines show means based on 5 to 19 MM. For each set 500 model combinations were generated. The blue (red) squares show selected multi-model mean projections for RCP45 (RCP85) based on a subset of models (n=5) that simulate the large-scale circulations in good faith.

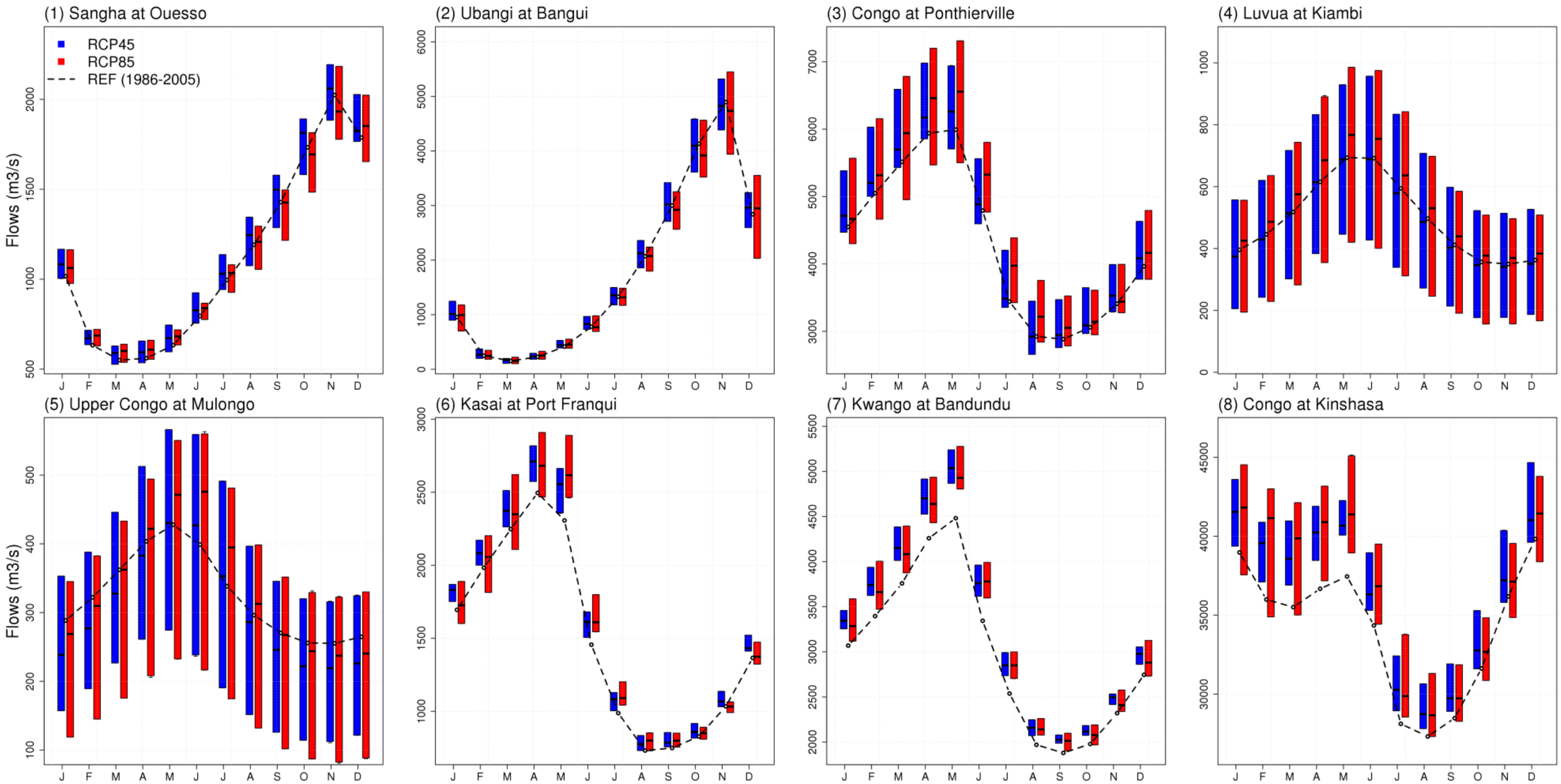

Figure S5 accessible stream flow hydrographs in the mid-term at selected locations shown in Figure 1A. Blue (red) bars show the inter-model variability. Dotted black line shows the hydrograph in the reference period (1986-2005). Figure numbers 1-8 coincide with the gage numbers in Figure 1A.

123

References

Arnold, J. G., R. Srinivasan, R. S. Muttiah, and J. R. Williams (1998), Large area hydrologic modeling and assessment part I: Model development, *Journal of the American Water Resources Association*, *34*(1), 73-89.

Bartholomé, E., and A. S. Belward (2005), GLC2000: a new approach to global land cover mapping from Earth observation data, *International Journal of Remote Sensing*, *26*(9), 1959-1977.

Bos, A. R., C. K. Kapasa, and P. A. M. Van Zwieten (2006), Update on the bathymetry of Lake Mweru (Zambia), with notes on water level fluctuations, *African Journal of Aquatic Science*, *31*(1), 145-150.

Burgis, M. J., and J. J. Symoens (Eds.) (1987), *African Wetlands and Shallow Water Bodies*, 650 pp., Institut Francais de Recherche Scientifique pour le Development en Cooperation, Paris.

Crul, R. C. M. (1992), Models for estimating potential fish yields of African inland waters*Rep. CIFA Occational Paper No. 16*, Food and Agricultural Organization of the United Nations, Rome, Italy.

FAO/IIASA (2009), Harmonized World Soil Database (version 1.1), in *Food and Agricultural Organization and IIASA*, edited, Rome, Italy and Laxenburg, Austria.

Hargreaves, G., and J. Riley (1985), Agricultural Benefits for Senegal River Basin, *Journal of Irrigation and Drainage Engineering*, *111*(2), 113-124.

Hawkins, R., T. Ward, D. Woodward, and J. Van Mullem (2009), *Curve Number Hydrology*, American Society of Civil Engineers, Reston, VA.

Kirchner, J. W. (2009), Catchments as simple dynamical systems: Catchment characterization, rainfall-runoff modeling, and doing hydrology backward, *Water Resour. Res.*, *45*.

Lamont, S. J., R. N. Eli, and J. J. Fletcher (2008), Continuous hydrologic models and curve numbers: A path forward, *Journal of Hydrologic Engineering*, *13*(7), 621-635.

Laraque, A., et al. (1998), Origin and function of a closed depression in equatorial humid zones: The Lake Tele in North Congo, *Journal of Hydrology*, *207*(3-4), 236-253.

Lehner, and P. Döll (2004), Development and validation of a global database of lakes, reservoirs and wetlands, *Journal of Hydrology*, *296*(1–4), 1-22.

Lehner, H., K. Verdin, and A. Jarvis (2008), New Global Hydrography Derived from Spaceborne Elevation Data, *Eos. Trans. AGU*, *89*(10).

Lempicka, M. (1971), Bilan hydrique du bassin du fleuve Zaire. *Rep.*, Office National de la Recherche et du Development, Kinshasa, DRC.

Magis, N. (1961), Nouvelle contribution à l'étude hydrobiologique des lacs de Mwadingusha, Koni et N'Zilo. *Rep.*, Université de Liège. Fondation de l'Université de Liège pour les recherches scientifiques en Afrique Centrale (FULREAC).

Nathan, R. J., and T. A. McMahon (1990), Evaluation of automated techniques for base flow and recession analyses, *Water Resources Research*, *26*(7), 1465-1473.

Neitsch, S. L., J. G. Arnold, J. R. Kiniry, and J. R. Williams (2011), Soil Water Assessment Tool - Theoretical Documentation - Version 2009*Rep. 406*, 647 pp, Texas Water Resources Institute, Texas A&M University, Temple, Texas.

Serruya, C., and U. Pollingher (1983), Africa, in *Lakes of the Warm Belt*, edited, pp. 131-284, Cambridge University Press, Cambridge, UK.

Sheffield, J., G. Goteti, and E. F. Wood (2006), Development of a 50-year high-resolution global dataset of meteorological forcings for land surface modeling, *Journal of Climate*, *19*(13), 3088-3111.

Tilzer, M. M., and C. Serruya (1990), *Large Lakes: Ecological Structure and Function*, 691 pp., Springer-Verlag, Berlin.

USDA Soil Conservation Service (1972), Section 4: Hydrology, in *National Engineering Handbook*, edited, United States Department of Agriculture (USDA), Washington, D.C.